# Nonaxial pearlike nuclear shapes

J. Skalski
*Sołtan Institute for Nuclear Studies, Hoża 69, PL-00 681 Warsaw, Poland*
(Received 10 September 1990)

We have extended the nuclear structure calculations to deformations that break both axial and reflection symmetry. The deformation energy has been calculated within the Strutinsky method with the Woods-Saxon mean field for systems that show signatures of octupole-deformed ground states. In well octupole-deformed light actinides, and in the neutron-rich heavy-barium region, the octupole minima turn out to be rather well localized around axial symmetry. On the other hand, rather flat energy landscapes in nonaxiality degree of freedom are found in some $Z \approx N \approx 56$ nuclei. The effect is especially well pronounced in $^{64}$Ge.

## I. INTRODUCTION

The motivation of this work is the extension of nuclear deformation energy calculations to more general nuclear shapes, including those breaking both axial and reflection symmetry. Calculations including triaxial but reflection symmetric, or reflection asymmetric but axial shapes, are quite common nowadays. The former are performed in order to study transitional nuclei, the shape evolution at high spins, the fission process, etc. The latter were most relevant to fission, but recently the reflection-asymmetric deformation of nuclear shape was invoked as a possible explanation for characteristic features observed in the low-energy spectra in some nuclei. The most typical are low-lying rotational bands with alternating-parity spin states linked by enhanced $E1$ transitions, as observed in the light radium-thorium region; see, e.g., Ref. 1. Up to now such rotational bands have been also observed in neutron-rich nuclei around $^{146}$Ba (Ref. 2) and, at higher spin, in a few nuclides around $^{148}$Sm.[3] There are also some indications of octupole correlations in the $Z \approx N \approx 32$ region.[4] A simple shell-model argument gives $Z$ or $N$ equal to 34, 56, 88, or 134 as the particle numbers of systems where octupole correlations should be strong.[5,8] The deformed mean-field calculations indeed predict the reflection-asymmetric equilibrium shapes in radium-thorium and heavy-barium regions.[6–9] There is no *a priori* reason which would prevent the nuclei which are octupole-deformed at their ground states to become triaxial with increasing angular momentum. Similarly, there is no reason for a fissioning actinide nucleus not to penetrate all symmetry-breaking shapes on its way from the first (triaxial) to the second (mass-asymmetric) saddle. Therefore, the inclusion of triaxial and reflection-asymmetric deformations seems to be a rather natural improvement of the mean-field approach. As an additional motivation for enlarging the family of nuclear shapes, one can mention octupole instability in the superdeformed minimum, recently found in calculations for $^{152}$Dy.[10]

However, before going to high spins or extreme deformations of fission, it is reasonable to look for effects of triaxiality first in octupole-deformed nuclei. This is the aim of the present work.

Since nearly all symmetries of the mean field are broken and large matrices are involved, the relevant numerical calculations are rather time consuming. This is precisely the reason why such calculations were rather rare in the past. The first, up to our knowledge, Strutinsky calculation in which a nucleus was allowed to have triaxial, reflection-asymmetric shape has been performed in the context of fission for heavy nuclei at the second saddle-point deformation.[11] More recent calculations of possible nonaxial pearlike ground-state deformations in the mass region $220 \leq A \leq 230$ have been reported by Chasman and Ahmad.[12] Using the grid of deformation points near the octupole minima, they have found the slow increase of energy with $\gamma$ up to $\gamma \approx 15°$ for some radon, radium, and uranium isotopes (the minima were sometimes shifted toward small values of $\gamma \approx 7°$). The results of Ref. 12 have been obtained without taking into account the deformation of multipolarity five $\beta_5$. This deformation was later shown to interplay effectively with octupole distortion in producing deeper reflection-asymmetric minima.[13,14]

In this paper we extend the study of Ref. 12 by taking into account the deformation of multipolarity five. In addition to the light actinides, we consider the neutron-rich nuclei around $^{146}$Ba, the very neutron-poor nuclei around $^{112}$Ba ($Z \approx N \approx 56$), and the neutron-poor isotopes with $N \approx Z \approx 32$. The results are presented in the form of maps showing the Strutinsky energy dependence on nonaxiality and reflection-asymmetry degrees of freedom around the equilibrium quadrupole deformation.

## II. SHAPE PARAMETRIZATION

A study of an octupole shape requires in general a consideration of at least a seven-parameter family of deformations and implies that the mean field does not possess any spatial symmetry. In practical terms this leads to a repetitive diagonalization of complex matrices of large dimension. Since it still presents a serious computational effort, we take a less general approach by imposing some limitations on the class of considered shapes.

The general nuclear shape is defined via the equation of a nuclear surface:

 

$$R(\vartheta,\varphi)=c(\{\beta\})\left[1+\sum_{\lambda,\mu}\beta_{\lambda,\mu}Y_{\lambda,\mu}(\vartheta,\varphi)\right], \quad (1)$$

$\lambda=2,3,\ldots,\mu=-\lambda,\ldots,\lambda$. First, we assume, as was done in previous calculations concerning axially symmetric and octupole-deformed shapes,[15] that the mirror reflection in the *y-z* plane is a conserved symmetry. The operator which performs such a mirror reflection is given by $\mathcal{S}_1=\mathcal{P}\mathcal{R}_1^{-1}$, where $\mathcal{R}_1=\exp(-i\pi I_1)$, $I_1$ is the angular momentum component along the intrinsic *x* axis, and $\mathcal{P}$ is the spatial reflection. This implies that $\beta_{\lambda\mu}=\beta_{\lambda-\mu}$ for even $\mu$, and that $\beta_{\lambda\mu}=-\beta_{\lambda-\mu}$ for odd $\mu$.[15] Our second requirement is that Hamiltonian matrix elements are real. This can be achieved if one adds the second symmetry, which we choose to be the second mirror reflection in the *x-z* plane $\mathcal{S}_2=\mathcal{P}\mathcal{R}_2^{-1}$. We note that this implies that $\mathcal{R}_3=\exp(-i\pi I_3)$ is also the symmetry operator and that all $\beta_{\lambda\mu}=0$ for odd $\mu$. We are left with a family of shapes, [Eq. (1)] for which

$$\beta_{\lambda,\mu}=\begin{cases}0 & \text{for odd } \mu,\\ \beta_{\lambda,-\mu} & \text{for even } \mu\end{cases}. \quad (2)$$

These conditions mean that, in addition to axial deformation of arbitrary multipolarity, we can have terms like $Y_{22}+Y_{2\text{-}2}$, $Y_{32}+Y_{3\text{-}2}$, $Y_{42}+Y_{4\text{-}2}$, $Y_{44}+Y_{4\text{-}4}$, etc.

The number of deformation parameters in Eqs. (1) and (2) is 10 for $\lambda_{max}=5$, and 14 for $\lambda_{max}=6$. In this work we restrict ourselves to $\lambda_{max}=5$. In order to present our results in the form of maps showing the energy dependence on reflection asymmetry and triaxiality, we had to choose only two relevant combinations of $\beta_{\lambda\mu}$ as the independent coordinates and to fix or constrain all others. The practical requirement is that the resulting parametrization should reduce to the usual one in the limits of reflection symmetry and axial symmetry. Three hexadecapole deformation parameters $\beta_{40}$, $\beta_{42}=\beta_{4\text{-}2}$, and $\beta_{44}=\beta_{4\text{-}4}$ are reduced to a single one $\beta_4$ using the parametrization of Ref. 16,

$$\begin{aligned}\beta_{4,0}&=\beta_4(5\cos^2\gamma+1)/6,\\ \beta_{4,2}&=-(15/2)^{1/2}\beta_4\sin(2\gamma)/6, \quad (3)\\ \beta_{4,4}&=(35/2)^{1/2}\beta_4\sin^2\gamma/6,\end{aligned}$$

where $\gamma$ is the usual parameter of the nonaxial quadrupole deformation, $\beta_{22}=\beta_{2\text{-}2}=-(1/\sqrt{2})\beta\sin\gamma$. This parametrization was used in many previous Strutinsky energy calculations including nonaxial quadrupole and hexadecapole shapes; see, e.g., Ref. 17. The nonaxial deformation parameters of multipolarities three and five were put equal to zero, $\beta_{32}=\beta_{52}=\beta_{54}=0$. The values of $\beta$ and $\beta_4$ were fixed at their equilibrium values following from the previous axially symmetric energy minimizations[13] (performed within the same model). Finally, the deformation $\beta_5=\beta_{50}$ is taken as a constant fraction of $\beta_3$, where this fraction equals the one at the equilibrium point in the above-mentioned studies. As a result, the energy map is obtained in the effective $(\beta_3,\gamma)$ plane, which cuts the deformation space through the axially symmetric equilibrium point.

It is worth noting that for the nonzero deformation $\beta_3$ or $\beta_5$, the $\gamma$ values in the range 0°–180° correspond to different nuclear shapes (see the right part of Fig. 3). At $\gamma=0°$ and 180°, the parametrization [Eqs. (1)–(3)] gives a pearlike axially symmetric shape, *z* axis being the symmetry axis, with the even-multipolarity-shape component being prolate and oblate, respectively. At $\gamma=60°$ (120°) the octupole deformation is still aligned to the *z* axis, while the *x* (*y*) axis is the symmetry axis of the quadrupole-plus-hexadecapole-shape component which is oblate (prolate). Thus, for $0°<\gamma<180°$, the nuclear shape has no symmetry axis unless all odd-multipole deformations vanish. At $\gamma\approx120°$ and large quadrupole deformation $\beta$, we obtain for $\beta_3\neq0$ "bananalike" shapes discussed in Ref. 10. Finally, it has to be noted that the well-known modulo-60° invariance in $\gamma$ of the pure quadrupole shape, which is preserved by the hexadecapole terms given by Eq. (3), cannot be preserved when the reflection-asymmetric deformation is added.[18]

## III. METHOD OF CALCULATION

The smooth part of the nuclear energy has been calculated according to the Yukawa-plus-exponential prescription.[19] The single-particle field used here is a natural extension of the deformed Woods-Saxon potential of Ref. 20 to the shapes discussed above. The pairing contribution to the Strutinsky energy has been calculated within the BCS method, unless it is stated otherwise. The pairing strengths were taken from Ref. 21. Thus the results presented below are the generalization of the results of Ref. 13 to more general nuclear shapes.

## IV. RESULTS

It follows from Ref. 13 that nuclei with reflection-asymmetric minima in heavy-barium and radium-thorium regions have a rather large prolate-oblate (PO) energy difference. Thus one does not expect very $\gamma$-soft energy landscapes in these nuclei. We present results for $\gamma\leq60°$, which constitutes the wide neighborhood of octupole prolate minima.

### A. Radium-thorium region

In calculations of Ref. 13, the evolution of octupole minima in the radium-thorium region shows a characteristic pattern. For every even-*Z* element, from Rn to Cf, the lightest even-even isotope showing odd-multipolarity deformation has a small quadrupole deformation $\beta_2\approx0.085$. This value is smaller than the equilibrium $\beta_3$ value. These weakly deformed systems occur at $N=132$ for Rn and at $N=130$ for Ra and heavier elements. The equilibrium quadrupole deformation increases with *N*, but when $\beta_2^{eq}$ becomes larger than 0.15, the reflection-asymmetric minimum disappears (at $N=140$ in Rn and Ra, at $N=138$ in Th, and at $N=136$ for heavier elements). The deepest reflection-asymmetric minimum occurs at $N=134$ in Rn, at $N=132$ in Ra, Th, and U, and at $N=130$ for heavier elements.

In Fig. 1 the Strutinsky energy maps are shown for $^{218,220,222}$Ra isotopes. The first of these nuclei has the equilibrium octupole deformation as large as the quadru-

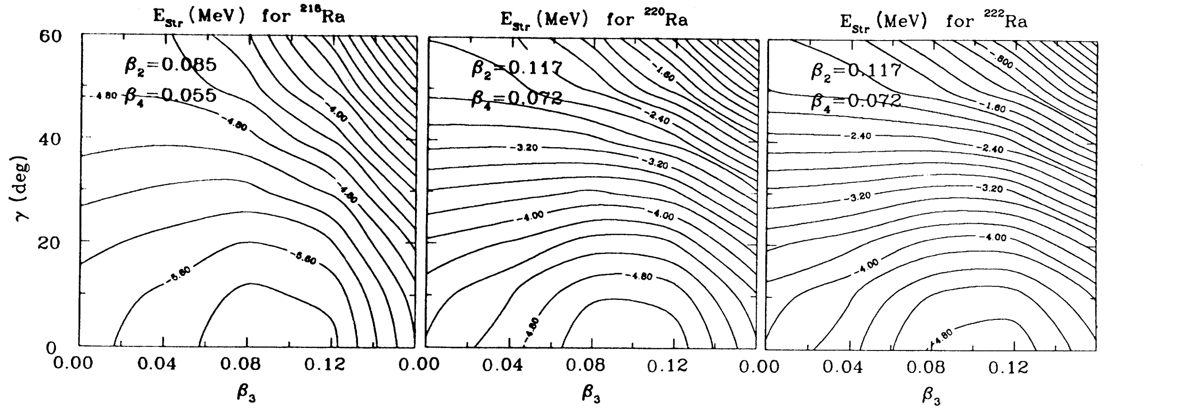


FIG. 1. Strutinsky energy in the $(\beta_3,\gamma)$ plane for three even-even radium isotopes $^{218-222}$Ra. The near-to-equilibrium values of $\beta_2,\beta_4$ displayed in figures and the relation $\beta_5=0.45\beta_3$ have been used in the calculations. The contour lines are 0.2 MeV apart.

pole one ($\beta_2=0.085$), while the two heavier ones are slightly more deformed ($\beta_2\approx0.12$). The deepest reflection-asymmetric minimum of all radium isotopes occurs in calculations for $^{220}$Ra, and the depth is close to 1 MeV. The minimum is nearly equally deep in $^{222}$Ra, while in $^{218}$Ra the spherical minimum is only about 100 keV above the octupole-deformed one[13] (since the point $\beta_3=\beta_5=0$ in Fig. 1 corresponds to a nonspherical deformation, the octupole minimum appears to be lower). The $\gamma$ stiffness increases with neutron number, especially between $N=130$ and 132, but even in $^{218}$Ra the minimum is quite localized at $\gamma=0°$. Near the minima, up to $\gamma=10°$, the increase in energy is moderate, e.g., 100 keV in $^{218}$Ra and 200 keV in $^{222}$Ra. For larger values of $\gamma$ the increase becomes quite steep; e.g., at the point $(\beta_3^{eq},20°)$ the increase in energy is already 300 keV in $^{218}$Ra and 800 keV in $^{222}$Ra. This increase results mainly from the shell correction term which strongly favors the $\gamma=0°$ shape. The Yukawa-plus-exponential model gives only slight (100–200 keV, depending on $\beta_3$) increase in energy from $\gamma=0°$ to 60°. The second feature visible in Fig. 1 for $^{220,222}$Ra is a nearly constant value of energy as a function of reflection asymmetry in the wide range of $25°\leq\gamma\leq45°$ up to $\beta_3\approx0.12$. This is not so for $^{218}$Ra. The landscapes calculated for thorium and uranium isotopes are similar to those shown for their isotones in Fig. 1. The less-deformed $N=130$ isotones are more $\gamma$ soft around the minimum. For radon the isotope with $N=132$ corresponds to $N=130$ isotones in heavier actinides.

### B. Heavy-barium region

In the heavy-barium region the equilibrium quadrupole deformation also increases with $N$.[13] The lightest isotopes with the reflection-asymmetric minimum are those with $N=86$, and their quadrupole deformations are larger than in the Ra-Th region.[13] The octupole minima disappear for $N=94$ (Xe), $N=96$ (Ba), $N=92$ (Ce), and $N=88$ (Nd). In Fig. 2 the corresponding maps are shown for the three barium isotopes $^{142,144,146}$Ba, which show the deepest calculated reflection-asymmetric minima in this region. These minima are shallower than for actinides, $^{146}$Ba having the deepest one of about 0.60 MeV. The results are rather similar to those for Ra-Th nuclei. The in-

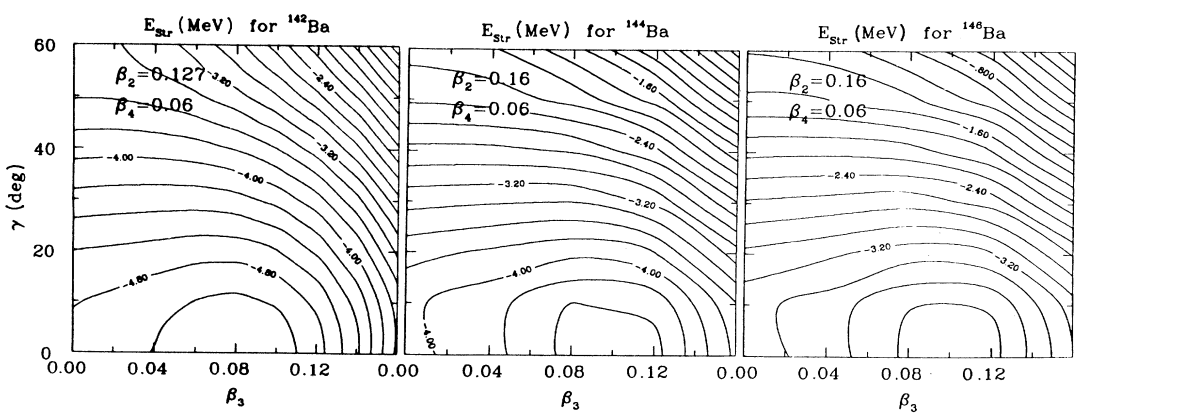


FIG. 2. As in Fig. 1, but for even-even $^{142-146}$Ba isotopes. The relation $\beta_5=0.5\beta_3$ has been used in the calculations. The contour line spacing is 0.2 MeV.

crease in $\gamma$ stiffness with the neutron number, mostly between $N=86$ and 88, is seen in Fig. 2. The increase in energy, when going from the minimum to $\gamma=10°$, is 100, 90, and 70 keV, for $N=86$, 88, and 90, respectively. At $(\beta_3^{eq},20°)$ the energy rises already by 450, 550, and 580 keV, respectively. The calculations carried out for heavy-xenon and -cerium isotopes show similar pattern.

### C. $Z \approx N \approx 56$ region

Recent calculations within the Strutinsky method[22] predict reflection-asymmetric minima for a few neutron-poor xenon and barium isotopes near $^{112}$Ba ($Z \approx N \approx 56$). The strongest octupole effect in this exotic region is found in calculations for particle number 56. In a majority of these nuclei, the energy difference between the reflection-asymmetric and reflection-symmetric minima does not exceed 300 keV. It is thus in the same range as in the heavy-barium region. The PO energy differences are rather large for nuclei with reflection-asymmetric minima in calculations employing the Woods-Saxon deformed potential. They decrease with the neutron number, but along with a disappearance of the octupole minima. A typical energy landscape in the $(\beta_3,\gamma)$ plane was shown in Ref. 23 for the very weakly octupolely deformed $^{114}$Xe isotope ($\beta_3^{eq} \approx 0.06$), for which the first experiments have been reported which try to establish the presence of octupole effects.[24] Although the PO energy difference is quite large for this nucleus, around 1.4 MeV the stiffness against nonaxiality around minimum is smaller than in the radium and barium regions. The energy rises above the minimum only by 40 keV at $\gamma=10°$, 200 keV at $\gamma=20°$, and by about 500 keV at $\gamma=30°$.

### D. Nucleus $^{64}$Ge

As representative of the $Z \approx N \approx 32$ region, we take the nucleus $^{64}$Ge, for which the most pronounced octupole correlations in this region have been found in calculations.[8,25] The energy map for this nucleus is shown in Fig. 3. The pairing energy was calculated including the particle number projection in this case. The pairing strengths $G_n = G_p = 19.8/A$ were used. The whole range of $\gamma$, from 0° to 180°, was covered in the calculation. The values of $\beta$ and $\beta_4$ have been changed linearly with $\gamma$ in order to interpolate between the octupole-deformed prolate ($\beta=0.167$, $\beta_4=-0.0325$) and reflection-symmetric oblate ($\beta=0.184$, $\beta_4=0.007$) minima found in Ref. 25. The relation $\beta_5=0.805\beta_3$, following from the ground-state deformations, has been used.

In order to visualize the change of nuclear shapes with $\gamma$, the cuts of the nuclear surface along one of the principal planes are shown in the right part of Fig. 3 for $\gamma=0°$, 60°, 120°, and 180°. For each $\gamma$ the reflection-asymmetric shape and the reflection-symmetric one, obtained by putting $\beta_3=\beta_5=0$, are shown. The cutting plane contains the $z$ axis and the axis of symmetry of the "reduced" reflection-symmetric shape.

Generally, the reflection-asymmetric deformation ($\beta_3 \geq 0.05$) is disfavored for shapes with $\gamma > 60°$. The structure at the $\beta_3=0$ axis is nearly repeated modulo-60°,

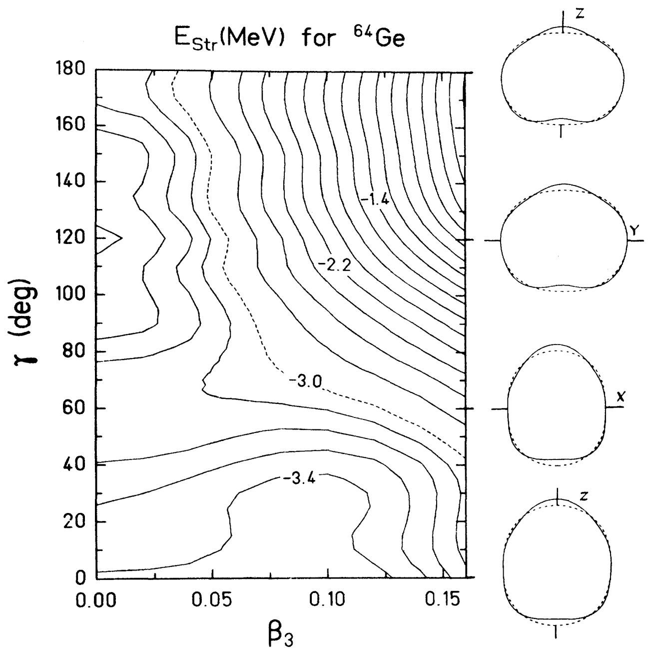


FIG. 3. Strutinsky energy for $^{64}$Ge. The whole range of $\gamma$ from 0° to 180° is covered. The deformations $\beta,\beta_4$ change linearly with $\gamma$, as described in text. The relation $\beta_5=0.805\beta_3$ is imposed. The contour line spacing is 0.1 MeV in the left lower and 0.2 MeV in the right upper parts of the map, respectively. The dashed contour line forms a border between these two parts. The nuclear shapes corresponding to $\beta=0.17$, $\beta_3=0.08$, $\beta_4=-0.03$, $\beta_5=0.06$, and $\gamma=0°$, 60°, 120°, and 180°, are visualized in the right part of the figure (solid line), together with "reduced" reflection-symmetric shapes, obtained by putting $\beta_3=\beta_5=0$ (dashed line), and their symmetry axes.

with hills at $\gamma=60°$ and 180° and valleys at $\gamma=0°$ and 120° (the structure is not strictly repeated since $\beta$ and $\beta_4$ change with $\gamma$). The PO energy difference is around 300 keV. In the range of $\gamma$ from 0° to 60°, we observe a relatively flat landscape, especially for $\beta_3$ around the equilibrium value $\beta_3^{eq}=0.08$, where the plateau in $\gamma$ (within 100 keV) extends to $\gamma \approx 30°$ (note that in Fig. 3, below the dashed contour line, the contour lines are only 100 keV apart). The calculations show that this softness with respect to nonaxiality and reflection asymmetry seen in the $(\beta_3,\gamma)$ plane extends to the neighborhood of the equilibrium values of $\beta$ and $\beta_4$.[23]

## V. DISCUSSION

We have found in our calculations, in which triaxial pearlike shapes were taken into account, that well-octupole-deformed nuclei from the light-actinide and heavy-barium regions show rather large stiffness against nonaxiality. One can expect that dynamical fluctuations in $\gamma$ are confined to the $\gamma$ range up to 10°–15°, where the increase in energy is moderate (100–200 keV). For larger values of $\gamma$ the energy rises steeply. The stiffness is smaller in very-neutron-poor xenon and barium isotopes near $^{112}$Ba for which calculations predict reflection-asymmetric deformation, yet undiscovered experimentally. The remarkable softness against both reflection-asymmetric and nonaxial deformations is predicted for $^{64}$Ge, which shows the shallow octupole minimum in the calculations.

What are the consequences of $\gamma$ softness in an octupole-deformed system, i.e., how should it manifest itself in the low-energy spectrum of the nucleus?

At first let us describe the extreme situation when the nuclear shape in the intrinsic frame, defined by Eqs. (1) and (2), is both nonaxial and reflection-asymmetric (e.g., it has nonzero equilibrium values of $\beta_{30}$ and $\beta_{22}=\beta_{2-2}$). One may thus say that the $D_2$ symmetry of the ellipsoidal shape is broken by the odd-multipole deformation, while the symmetries $\mathcal{R}_3$ and $\mathcal{S}_2=\mathcal{P}\mathcal{R}_2^{-1}$ are still conserved. Within the rigid-rotor model, on the intrinsic state of an even-even nucleus with the eigenvalues $r_3$ of $\mathcal{R}_3$ and $s_2$ of $\mathcal{S}_2$, the rotational spectrum is built with the rotational wave functions belonging to the $D_2$ representations with the same eigenvalue of $r_3$ and both eigenvalues $r_2$ of $\mathcal{R}_2$, $r_2=\pm 1$ (parity is determined by $\pi=r_2 s_2$).[26] Taking the intrinsic ground state with $r_3=s_2=1$, we get the rotational spectrum containing positive-parity states (with $r_2=1$) with the following spins and in numbers given by the superscript: $0^1,2^2,3^1,4^3,5^2,\ldots$; and negative-parity states (with $r_2=-1$) with spins and numbers of states: $1^1,2^1,3^2,4^2,5^3,\ldots$. In the limit of axial symmetry, only the alternating-parity band survives as the ground-state band. The characteristic low-energy features of this rich rotational structure would be the exceptionally low-lying $\gamma$-like band with its parity-doublet band in addition to the alternating-parity octupolelike ground-state band, and the enhanced $E2$ transitions from opposite-parity $\gamma$-like bands to the alternating-parity ground-state band. Furthermore, such a spectrum should contain many low-lying good-$K$-like bands with strong interband $E2$ transitions.

Now consider an octupole-deformed system with $\gamma$ softness, but without any stable nonaxial deformation. In such a system we should expect the low-lying $\gamma$-vibrational band. Its parity-doublet partner ($I^\pi=2^-,3^-,4^-,\ldots$) may be shifted up in energy by the interaction with the nonaxial octupole one-phonon state which carries the same $K$ number and is expected at low energy. Indeed, in the actinide region the low-lying $I^\pi=2^-$ states have been observed and interpreted as the one-octupole-phonon states with $K^\pi=2^-$.[27] Approaching the limit of the $\gamma$ instability, the system should show features more similar to the ones discussed above for stable nonaxiality, in particular, relatively many low-lying bands (resulting from the superposition of the low-energy $\gamma$ vibration with other low-lying excitations), and the enhanced $E2$ interband transitions.

Unfortunately, not much is known about the $\gamma$ bands in octupole-deformed nuclei. Very often only one state, interpreted as a bandhead, is known. Moreover, the nuclei of interest are weakly deformed, which makes the interpretation of bands more difficult. With these reservations in mind, we can compare the energies of the quasi $\gamma$ bandheads, taken from Ref. 28, to the energies of the lowest negative-parity states in all four studied regions of octupole nuclei. In $^{224}$Ra the $\gamma$-vibration energy, 965 keV, is more than 4 times larger than that of the lowest negative-parity state; in $^{144}$Ba (1316 vs 759 keV) and $^{146}$Ba (1115 vs 739 keV), it is less than 2 times larger, but it is less than 2 times smaller in $^{114}$Xe [1148 vs 1798 keV (Ref. 24)], $^{66}$Ge (1693 vs 2798 keV), and $^{68}$Ge (1777 vs 2649 keV). These data are not inconsistent with our results showing increasing importance of nonaxial correlations for lighter octupole-deformed systems.

The enhanced interband $E2$ transitions are the characteristic feature of $\gamma$ softness or $\gamma$ deformation also in odd nuclei, provided that they do not follow from the Coriolis coupling. Such transitions have been analyzed in Ref. 12. The transitions of a few single particle units found in $^{223}$Ra and $^{225}$Ra were proposed as the evidence for nonaxial correlations in these nuclei. It follows from our study that such transitions should be even stronger in the regions of lighter nuclei showing octupole correlations.

## ACKNOWLEDGMENTS

The author would like to thank W. Nazarewicz and J. Dobaczewski for their remarks and comments. The kind hospitality of the GSI, Darmstadt, where a part of the work has been done, is gratefully acknowledged. This work has been supported by Polish Ministry of National Education, Grant No. CPBP 01.09.

[1] J. Zylicz, in *Proceedings of the International Conference on Nuclear Structure, Reactions and Symmetries, Dubrovnik, 1986,* edited by R. A. Meyer and V. Paar (World Scientific, Singapore, 1986), Vol. 1, p. 79.

[2] W. R. Phillips, I. Ahmad, H. Emling, R. Holzmann, R. V. F. Janssens, T. -L. Khoo, and M. W. Drigert, Phys. Rev. Lett. **57**, 3257 (1986); Phys. Lett. B **212**, 402 (1988).

[3] W. Urban, R. M. Lieder, W. Gast, G. Hebbinghaus, A. Krämer-Flecken, K. P. Blume, and H. Hübel, Phys. Lett. B **185**, 331 (1987); *ibid.* **200**, 424 (1988).

[4] J. Görres, T. Chapuran, D. P. Balamuth, and J. W. Arrison, Phys. Rev. Lett. **58**, 662 (1987).

[5] G. A. Leander, in *Nuclear Structure 1985,* edited by R. A. Broglia, G. B. Hagemann, and B. Herskind (North-Holland, Amsterdam, 1985), p. 249; W. Nazarewicz, in *ibid.*, p. 263.

[6] P. Möller and J. R. Nix, Nucl. Phys. **A361**, 117 (1981).

[7] G. A. Leander, R. K. Sheline, P. Möller, P. Olanders, I. Ragnarsson, and A. J. Sierk, Nucl. Phys. **A388**, 452 (1982).

[8] W. Nazarewicz, P. Olanders, I. Ragnarsson, J. Dudek, G. A. Leander, P. Möller, and E. Ruchowska, Nucl. Phys. **A429**,

269 (1984).
[9]P. Bonche, P. H. Heenen, H. Flocard, and D. Vautherin, Phys. Lett. **175B**, 387 (1986).
[10]J. Dudek, in *The Variety of Nuclear Shapes,* edited by J. D. Garret *et al.* (World Scientific, Singapore, 1988), p. 195.
[11]S. Åberg, S. E. Larsson, P. Möller, S. G. Nilsson, G. Leander, and I. Ragnarsson, in *Physics and Chemistry of Fission, 1979,* edited by IAEA (IAEA, Vienna, 1980), Vol. I, p. 303.
[12]R. R. Chasman and I. Ahmad, Phys. Lett B **182**, 261 (1986).
[13]A. Sobiczewski, Z. Patyk, S. Cwiok, and P. Rozmej, Nucl. Phys. **A485**, 16 (1988).
[14]S. Cwiok and W. Nazarewicz, Nucl. Phys. **A496**, 367 (1989).
[15]W. Nazarewicz and P. Olanders, Nucl. Phys. **A441**, 420 (1985).
[16]S. G. Rohoziński and A. Sobiczewski, Acta Phys. Pol. B **12**, 1001 (1981).
[17]W. Nazarewicz, J. Dudek, R. Bengtsson, T. Bengtsson, and I. Ragnarsson, Nucl. Phys. **A435**, 397 (1985).
[18]S. G. Rohoziński, M. Gajda, and W. Greiner, J. Phys. G **8**, 787 (1982).
[19]H. J. Krappe, J. R. Nix, and A. J. Sierk, Phys. Rev. C **20**, 992 (1979).
[20]S. Cwiok, J. Dudek, W. Nazarewicz, J. Skalski, and T. Werner, Comput. Phys. Commun. **46**, 379 (1987).
[21]J. Dudek, A. Majhofer, and J. Skalski, J. Phys. G **6**, 447 (1981).
[22]J. Skalski, Phys. Lett. B **238**, 6 (1990).
[23]J. Skalski, in *Proceedings of the XXIV Zakopane School on Physics,* edited by J. Styczeń and Z. Stachura (World Scientific, Singapore, 1990), Vol. 1, p. 299.
[24]P. A. Butler, in *Heavy Ions in Nuclear and Atomic Physics,* edited by Z. Wilhelmi and G. Szeflińska (Hilger, London, 1989), p. 295.
[25]S. Cwiok and W. Nazarewicz (unpublished).
[26]A. Bohr and B. R. Mottelson, *Nuclear Structure* (Benjamin, New York, 1975), Vol. 2
[27]R. R. Chasman, in *Proceedings of the International Conference on Nuclear Structure, Reactions and Symmetries, Dubrovnik, 1986,* edited by R. A. Meyer and V. Paar (World Scientific, Singapore, 1986), Vol. 1, p. 5.
[28]M. Sakai, At. Data Nucl. Data Tables **31**, 399 (1984).